

# Evaluation of Calibration Procedures for Optical See-Through Head-Mounted Displays

Arthur Tang, Ji Zhou, Charles Owen

Media Entertainment Technology Laboratory  
Michigan State University, East Lansing, Michigan

tangkwo1@msu.edu, zhouji1@cse.msu.edu, cbowen@cse.msu.edu

## Abstract

Optical see-through head-mounted displays (HMDs) are less commonly used because they are difficult to accurately calibrate. In this article, we report a user study to compare the accuracy of 4 variants of the SPAAM calibration method. Among the 4 variants, Stylus-marker calibration, where the user aligns a crosshair projected in the HMD with a tracked stylus tip, achieved the most accurate result. A decomposition and analysis of the calibration matrices from the trials is performed and the characteristics of the computed calibration matrices are examined. A physiological engineering point of view is also discussed to explain why calibrating optical see-through HMD is so difficult for users.

## 1. Introduction

The term Augmented Reality (AR) is used to describe systems that blend computer generated virtual objects or environments with real environments [1-3]. A typical AR system for enhanced vision uses a head-mounted display (HMD) to compose the real and virtual environment in a user's visual field. There are two major types of head-mounted displays for AR systems: optical see-through HMDs and video see-through HMDs. A video see-through HMD consists of an opaque HMD and one or two small video cameras mounted on the HMD. Real time video streams from the cameras are combined with computer-generated graphics and displayed inside the opaque HMD. An optical see-through HMD overlays computer graphics on the real environment using a partially transmissive half-silvered mirror.

There are advantages and disadvantages to both display technologies (see a recent comprehensive review of display technologies for AR systems done by Rolland and Fuch [4]). The recent trend in universities and industrial research laboratories is to use video see-through HMD to implement research projects and prototypes. One of the reasons for this trend is that

systems can use video signals from the HMD for video-based head tracking so there is no need to acquire an additional motion tracking system [5]. Also, video see-through HMD's are relatively easy to calibrate, since the computer can directly analyze the image as it will be presented to the user. The composition occurs directly on that image.

Display calibration refers to the alignment between the virtual world displayed in the HMD and the physical world. Calibration of video see-through HMDs can be done using tradition camera calibration procedures, where real world points are simply located visually in the imagery. Optical see-through HMDs are less commonly used because they are much more difficult to calibrate and it is hard to assess the accuracy of the calibration. The composition of the real content as seen through the display and the overlay content as reflected by the half-silvered mirror occurs within the eye. It is not practical to capture this image as seen by the eye, so the correspondences between points in the real world, points in the HMD display, and locations on the retina cannot be directly measured. Unlike video see-through HMD calibration, optical see-through HMDs have to be calibrated online with the user indicating the correspondence between real world points and display points. This human-computer interaction process is highly user dependent. Hence this difficulty of calibration for optical see-through HMD is a major obstacle for its practical usage.

The study presented in this article explores human factors in different variants of the SPAAM calibration algorithm for optical see-through HMD, and why calibration for optical see-through displays is difficult for users.

## 2. Optical See-Through Head-Mounted Display Calibration

In a typical AR system, a tracking system provides information about the position and orientation of a user's head relative to the source of the tracking system. In order for the computer graphics to merge with the real

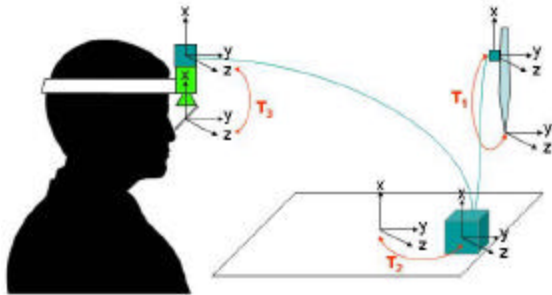


Figure 1. Transformation between different coordinate system.

world in a spatially meaningful way, a series of calibrations is required. These calibrations allow the placement of graphics in the computer display so as to correspond with real elements as seen through the display.

## 2.1 Overview of Tracking Requirements

Typically, three calibration procedures are necessary to obtain the parameters of these geometric relations: pointer calibration, workspace calibration, and display calibration. Pointer calibration determines a geometric transformation from the marker of a tracking system attached to the pointer to the tip of the pointer (Transformation  $T_1$  in Figure 1). Pointer calibration is necessary because we need to pick points in the workspace to align it with the virtual world in workspace calibration. Workspace calibration is the alignment of the real world coordinate system to the tracker coordinate system (Transformation  $T_2$  in Figure 1). With a calibrated pointer, we can pick points in the real world and estimate a rigid body or affine transformation to the equivalent points in the virtual world. Display calibration refers to a method to estimate the projective transformation that applies to the virtual objects displayed on the HMD, so that the virtual objects are displayed in the correct position in the see-through HMD and appear to be spatially registered with the real world (Transformation  $T_3$  in Figure 1).

## 2.2 Display Calibration

Several display calibration methods for see-through HMD have been developed by various researchers. Azuma mentioned two approaches to calibrate optical see-through HMD in his dissertation [6]: a non-systematic approach consisting of aligning a virtual object with a real object, and a systematic approach



Figure 2. The system setup.

using a boresight method that aligns different markers in the real world to a projection in the see-through HMD. These approaches require a trained user, and usually do not achieve robust results. Tuceryan and Navab developed a display calibration method called Single point active alignment method (SPAAM) [7]. This is a less mentally demanding method than the previous approaches since the calibration procedure only involves aligning a single point displayed in the HMD with a point in the real world repeatedly. An extension of the SPAAM method was developed by Genc *et al.* for stereo display calibration [8]. The procedure used by this method involves repeatedly aligning a 3D circular disc projected in the HMD to a circle in the workspace so that the two radii match and the centers are aligned.

## 3. Usability Study for Different Calibration Methods

Some of our initial informal experimentation and evaluation of optical see-through HMD calibration methods indicated that human factors contribute significantly to display calibration error. Calibration procedures are considered complex and mentally demanding for novice users. There are also physiological factors (which we will discuss in Section 5.3) that contribute to inaccuracy in the head-pointing task of some of the common calibration procedures. We designed a usability study in order to compare different calibration methods for optical see-through HMD. This study explored factors that affect display calibration accuracy, and exposed weaknesses of different variants of the SPAAM display calibration procedures.

### 3.1 Methodology

A between-subjects experiment with four treatment conditions was conducted: (1) SPAAM, (2) Depth-SPAAM (SPAAM modified to force point depth), (3) Stereo-SPAAM, and (4) Stylus-Mark calibration.

### 3.2 Experimental Setup

We implemented the calibration procedures for all 4 treatment conditions using the ImageTclAR Toolkit developed by the Media and Entertainment Technologies Laboratory at Michigan State University [9]. Head movement was tracked using an Ascension Flock of Birds 6 degree of freedom magnetic motion tracking system. This tracking system was also used to track the stylus in treatment condition 4. The optical see-through head-mounted display used is the Sony Glasstron LDI-100B. The display was modified to remove the liquid crystal shutter, significantly increasing the optical transmission of the display. The display resolution was 800 by 600 pixels and all calibrations were done in stereo. A photograph of the system is shown in Figure 2.

**3.2.1 Treatment Condition 1: SPAAM.** The SPAAM calibration method [7] is used in this condition, and each eye is calibrated separately, though the points are captured in alternating fashion between the eyes. The calibration procedure requires the subject to align 18 crosshairs presented in the HMD sequentially to a crosshair located in the middle of the workspace (nine positions for each eye). The nine positions and sequence of appearance on the HMD were predefined (Figure 3), and the crosshair was presented to one of the user's eyes at a time (i.e. the first crosshair was presented to the left eye at position 1, the second crosshair was presented to the right eye at position 1, the third crosshair was presented to the left eye at position 2, and so on). The subject were also instructed to move their body forward and backward to acquire positions at different depths during the calibration procedure so that the points collected have different depth and are not coplanar. A problem with any calibration method trained on coplanar points is that alternative solutions with different blends of field of view and object difference are equally valid. Hence, all of the presented methods will fail if only coplanar data is supplied.

**3.2.2 Treatment Condition 2: Depth-SPAAM.** The Depth-SPAAM calibration procedure is a special condition of the SPAAM procedure, in which the system forces the user to move forward and backward when collecting different data points. The user interface for the

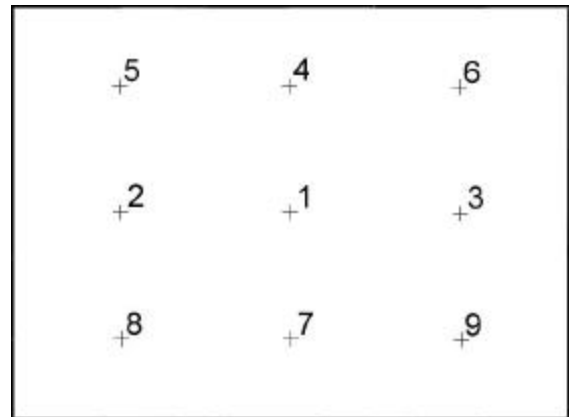


Figure 3. Nine positions are predefined in the optical HMD projection. Crosshair appears in sequence on either the left or the right eye on the HMD.

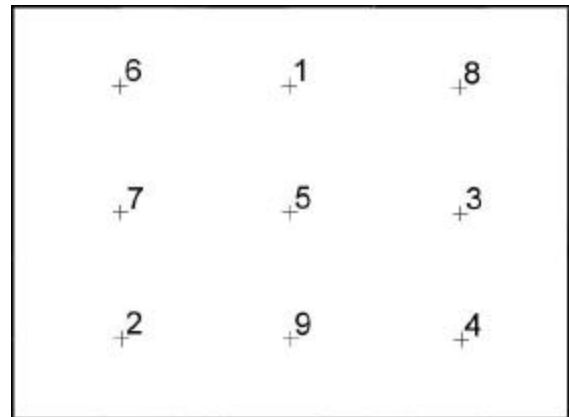


Figure 4. Predefined depth for each of the position in treatment conditions 2, 3, and 4.

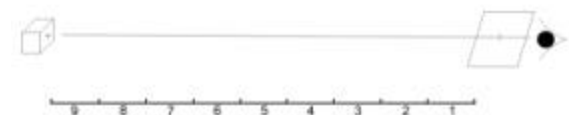


Figure 5. Participants were to align a crosshair displayed on the optical see-through HMD to a crosshair in the workspace. In condition 2, 3, and 4, participants had to move with a predefined depth for the correspondent position.

procedure instructs users to move their head forwards and backwards and will not accept data points that do not span a preselected range. Each of the nine positions was predefined with a depth value using a Magic Square (Figure 4). For example, position 1 (the center point, as defined in figure 3) is predefined with a depth value of 5 (as defined in figure 4). The user interface allows for the

specification of a near and far distance that is comfortable for the user and all distances are relative to this range. Distance 1 is closest and distance 9 is farthest. The advantage of the magic square pattern is that all columns, rows, and diagonals add to the same value (15). Because of this, the average calibration depth for every row, column, and diagonal is the same. This allows the calibration to have statistically balanced data. Participants had to move within the predefined depth and align the projected virtual crosshair to the physical crosshair in the workspace. The user interface forces the depth to ensure the SPAAM calibration algorithm has enough depth information.

**3.2.3 Treatment Condition 3: Stereo-SPAAM.** In the Stereo-SPAAM calibration procedure, a 3D circular disc was presented in the HMD by rendering two circles in each eye with some stereo disparity. The subject was instructed to align this circular disc so that it appears to be floating in front of the subject superimposed on a circle in the middle of the workspace with the two radii matching and the centers aligned. The same Magic Square approach in section 3.2.2 is implemented to ensure that the points collected have enough depth information for the stereo-SPAAM calibration algorithm, though the depth information is now used to force stereo disparity. This routine is repeated nine times and the locations of the discs are the same as treatment conditions 1 and 2.

**3.2.4 Treatment Condition 4: Stylus-mark calibration.** The Stylus-mark calibration procedure is a special version of the Depth-SPAAM procedure, where a crosshair in the display is touched by the user using a tracked stylus. This method was previously implemented by Fuhrmann et. al. [10, 11]. Participants held the stylus in their hand and were free to move the stylus during the alignment. The same Magic Square approach in section 3.2.2 was implemented to ensure that the points collected have enough depth information for the SPAAM calibration algorithm.

### 3.3 Measurement

Two measurements were taken for each trial: time of completion and calibration error. Quantitative calibration error was measured online using the method developed by McGarrity et. al. [12, 13]. Subjects repeated the experimental procedure two times, and the mean values of the two trials were taken as a final measurement.

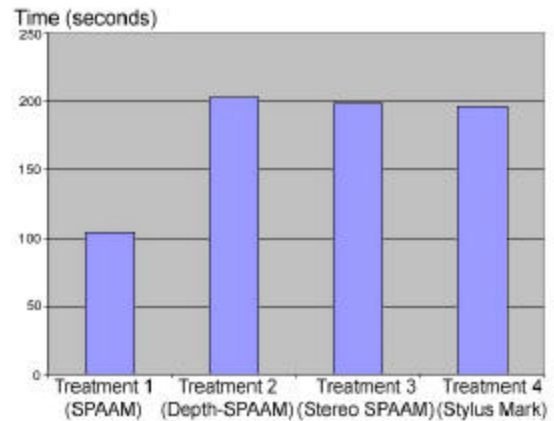


Figure 6. Average time of completion in each treatment conditions.

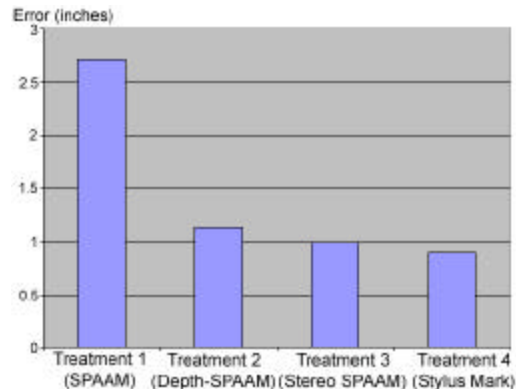


Figure 7. Average error in each treatment conditions.

### 3.4 Experimental Procedure

Participants were first briefed about the whole experimental procedure, and were randomly assigned to one of the four treatment conditions. Participants then proceeded to the calibration procedure followed by the error evaluation procedure. The calibration procedure and error evaluation procedure was repeated after participants took a brief break.

### 4. Result

21 undergraduate and graduate level university students volunteered to participate in the study. Most of them have no previous experience in any AR environment, and have no experience in HMD calibration. There were 5 participants assigned to each of treatment condition 1, 3, and 4, and 6 participants assigned to treatment condition 2.

## 4.1 Descriptive Statistic

Figure 6 shows the mean time of completion of the calibration procedure in seconds for each treatment condition. It shows that treatment condition 1 (SPAAM) has the shortest time of completion among the 4 treatment conditions, and treatment condition 2 (Depth-SPAAM) has the longest time of completion. Figure 7 shows the mean error of the calibration in inches for each treatment condition. The statistic shows that treatment condition 4 (Stylus-Mark) has the least error among the 4 treatment conditions, and treatment condition 1 (SPAAM) has the largest error. Also illustrated is the significant different depth management makes in the calibration process.

## 4.2 Decomposition Analysis

In all cases the calibration was computed as a best-affine projection matrix. It is useful to examine the characteristics of the computed calibration matrices as a way to understand why calibrations fail or achieve inconsistent results. We performed a decomposition of the calibration matrices from the trials and analyzed the data. The goal of this analysis was to determine the characteristics of the computed matrices so as to better understand how the distribution of points is and is not effectively determining valid matrices and to determine the effect of human error in the process.

A projection matrix  $M$  can be expressed in terms of the camera intrinsic and extrinsic parameters:

	Left $\mu$	Left $\sigma$	Right $\mu$	Right $\sigma$
Top 10	3.96	1.41	4.32	0.27
Top 20	3.83	1.53	4.43	0.90
All	3.51	3.76	3.46	2.02

Table 1. Mean and standard deviation for the focal length in inches for each eye

	Left $\mu$	Left $\sigma$	Right $\mu$	Right $\sigma$
Top 10	0.78	0.05	0.80	0.06
Top 20	0.77	0.13	0.76	0.10
All	0.90	0.37	1.14	1.32

Table 2. Computed aspect ratio for each eye.

	Left $\mu$	Left $\sigma$	Right $\mu$	Right $\sigma$
Top 10	90.69	7.55	91.91	1.23
Top 20	87.75	11.37	91.10	4.63
All	87.43	17.90	89.85	19.89

Table 3. Skew between the horizontal and vertical axis of the projection plane for each eye.

$$C = \mathbf{r} \begin{pmatrix} \mathbf{a}r_1^T - \mathbf{a} \cot \mathbf{q} r_2^T + u_0 r_3^T & at_x - \mathbf{a} \cot \mathbf{q} t_y + u_0 t_z \\ \frac{\mathbf{b}}{\sin \mathbf{q}} r_2^T + v_0 r_3^T & \frac{\mathbf{b}}{\sin \mathbf{q}} t_y + v_0 t_z \\ r_3^T & t_z \end{pmatrix}$$

In this equation,  $t_x$ ,  $t_y$ , and  $t_z$  are the coordinates of the camera center of projection. The three vectors  $r_1$ ,  $r_2$ , and  $r_3$  are the rows of a rotation matrix  $R$  which represents the orientation of the world relative to the camera coordinate system.  $(u_0, v_0)$  is the camera principle point, the point on the projection plane pierced by the camera  $-Z$  axis.  $(\alpha, \beta)$  is a scaling factor in two dimensions and an element of the window-to-viewport transformation for the camera system.  $\theta$  is any skew angle between the vertical and horizontal axis.  $\rho$  is an arbitrary scaling factor dependent upon the method used to compute the projection matrix.

Various methods exist for decomposition of a

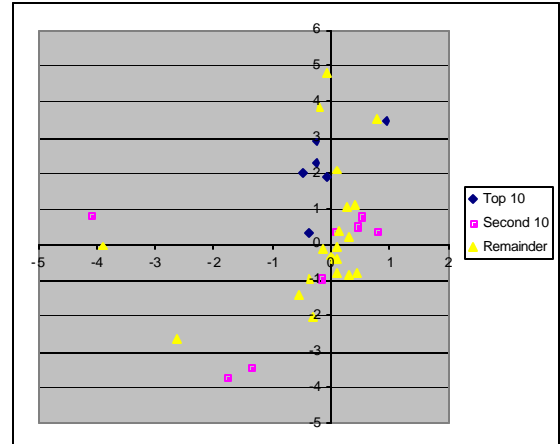


Figure 8 - Left eye principle point

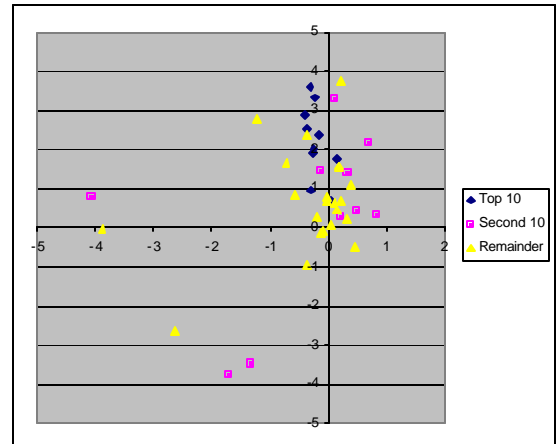


Figure 9 - Right eye principle point

computed camera calibration matrix into the intrinsic and extrinsic parameters. We implemented a decomposition method and analyzed the results. The horizontal scaling factor  $\alpha$  in the above equations is based on a normalized focal distance of -1. This factor is effectively identical to focal length if a projection plane with a normalized area is substituted. Table 1 presents the mean and standard deviation for the focal length in inches for each eye. The results are presented for the top 10 and top 20 ranked results as determined by the performance evaluation (as described in section 3.3) and for all users.

This data illustrates the variance is much less for more accurate calibrations. It also illustrates a common thread discovered throughout the calibration process. The right eye data exhibits consistently smaller variance than the left eye. The evaluation was based on stereovision and did not distinguish between good and bad eyes. But, the data analysis is done independently.

The ratio  $\alpha/\beta$  indicates the aspect ratio of the projection plane. This is an indication of pixel squareness. In our implementation, pixel locations on the display have been normalized to the range [-1, 1] in both dimensions. Hence, the square pixels of the Glasstron display have an aspect ratio in normalized values of 600/800 or 0.75. Table 2 lists the aspect ratio as computed for each eye. It is clear that variance increases in all cases as the accuracy of the computed calibration decreases.

The value  $\theta$  is any skew between the horizontal and vertical axis of the projection plane. This value should be 90 degrees for the Glasstron display. Table 3 indicates the computed results.

The values  $(u_0, v_0)$  are the camera principle point. If the center of focus of the eye is exactly behind the center of the display and along a vector orthogonal to the display projection plane, this value will be (0,0). In practice, this value captures both any offset of the eye relative to the display and any display tilt. Figure 8 and Figure 9 illustrate the principle points for the left and right eyes. The clearly visible vertical groupings in these images are indicative of tilting the display on its hinge. Different users place the display on the head in slightly different ways. The outlier points are from calibrations that were drastically wrong and an indication that bounding the free parameters may improve the performance of calibration computations in the presence of bad data. The common location of the outliers is likely a numerical artifact of the failure to compute a valid calibration.

It is clear that calibration failures tend to cause wide-ranging variations in the free parameters. Limiting the range of free parameters may help to improve the

accuracy of computed calibrations in the presence of noisy data and human errors in the process. The focal length does not seem to vary significantly among users and can likely be fixed. The aspect ratio is fixed by the HMD. The principle point is predominantly an indicator of the display angle, which is common between the eyes; hence a stereo calibration linking this parameter may improve calibration performance.

## 5. Discussion

The goal of this study was primarily to provide input for improvements in the display calibration process. From a human computer interface standpoint, the process is routinely reported as tedious and dull and this is often reflected in the performance. It is fundamentally a targeting task and dependent on the quality of the user's pointing skills. This section discusses some of the factors discovered in this process and how these factors can be utilized to produce a better calibration algorithm.

### 5.1 Time of completion

Among the 4 treatment conditions, the average time of completion of treatment condition 1 (SPAAM) is significantly shorter (104.7 seconds) than the other 3 treatment conditions. However, treatment condition 1 also has the largest average amount of error among the 4 treatment conditions (2.72 inches). The short calibration time illustrate that this is the most intuitive and straightforward calibration method, requiring the minimum training to perform, but it performs worse in term of accuracy. Much of this error appears to be due to the lack of control over depth, which does not ensure a good range of calibration point depths.

### 5.2 Calibration Accuracy

Among the 4 treatment conditions, treatment 4 (Stylus-marker) has the most accurate calibration on average (0.91 inches). We originally hypothesized that the hand-eye coordination task in this treatment would complicate the procedure and would result in a lower accuracy. We hypothesize that this result is because of the minimizing the effect of extrinsic head movement caused by movement of the body. We will elaborate this hypothesis in the section 5.3.

### 5.3 Head Pointing as an Input Method

All 4 calibration methods involve a head pointing task to align a projection in the HMD to something in the workspace. There is a body of research in input device

exploring using head motion as an input method [14, 15]. A measurement of difficulty of input devices for a pointing task can be calculated using Fitts's Index of Difficulty [16]. The Fitts's Index of Difficulty can be used to compare performance of the same pointing task using different input devices (e.g. traditional mouse versus headpointing). Experimental data by Langolf [17] shows that the neck muscles have the highest Index of Difficulty (i.e. most difficulty) among arm muscles, wrist muscles, and finger muscles. Card *et al.* also showed that the "head-mouse" is not precise enough for a character pointing task in text editing because it has "too little muscle bandwidth for the precision" [18]. In an optical see-through calibration procedure, we are attempting to achieve a 1-pixel precision head pointing task. This corresponds to approximately a 0.05 degree precision of head rotation on a 800x600 display at normal working distance. Physiologically, muscles of the neck and head do not provide the level of precision necessary to achieve a 1-pixel head pointing task. However, this angular precision of the alignment task can be improved by incorporating hand, wrist and finger motion, as in treatment condition 4.

Anatomically, the neck-head muscles system is quite strong and head motions are relatively steady. However, most participants reported that it is hard to hold their head still when they are aligning the crosshairs. Although intrinsic movement of the neck and head (movement of the head relative to the body) is rather stable, it is the extrinsic movement of the body (movement of the head caused by the movement of the body) that causes the position of the head swinging relative to the workbench. Some participants incorporated a technique of leaning on the workbench or the chair to help stabilize the body during the alignment. In treatment condition 4, we believe that the effect of extrinsic movement of the body is reduced because participants held the stylus in their hand. Head motion was limited to fixing the head relative to the body and any body motion was transfer both to the head and the body simultaneously.

## 5.4 Learning Effect

We observe that participants perform faster in the second trial than in the first trial, but not more accurately. Even though an experiment with 2 trials is not sufficient for studying learning effects, we observe a trend for which that the time of calibration can be improved in short term, but not calibration accuracy. This seems to indicate that the task is simple enough not to require extensive training, but that users are unlikely to improve in performance over time. This has, indeed,

been seen to be the case, where experienced users in the lab do not seem to significantly improve their calibration ability over time.

## 5.5 Left Eye Exhibits Higher Error Consistently

The decomposition analysis illustrated that the data for the right eye exhibits consistently smaller variance than the left eye. This indicates that the calibration on the left eye is less consistent and probably less accurate than the right eye. This characteristic is believed to be due to the fact that the calibration user interface was structured to present points in a left-right sequence.

In treatment condition 1, participants were asked to move forward and backward after they completed the alignment of a left-right pair, and in treatment condition 2 and 4, participants were forced to move within a range of location for every left-right pair. The alignments of the left eye always follow a drastic body movement, while the body is relatively stable before the alignments of the right eye. So the alignments of the left eye suffer more from the error caused by extrinsic body movement. We recommend either randomizing the sequence of appearance of the crosshair to the left and to the right eye or changing the alternative to left/right/right/left, so this source of error would be distributed evenly among the two eyes. Note that the Stereo-SPAAM calibration does not favor either eye and that data was included in this calculation. A large sample of the Stereo-SPAAM calibration data would need to be collected for accurate determination of any eye-favoring for that method.

## 6. Conclusion

Human factors contribute to a significant amount of calibration error and different calibration procedures for the same calibration algorithm yields significantly different accuracy. Based on our study, we suggest the following guideline for designing optical see-through HMD calibration procedures:

1. Calibration procedures should not rely purely on head pointing.
2. Extrinsic body movement should be minimized to keep the head stabilized.
3. The sequence of data collection for the two eyes also needs to be carefully considered when designing calibration procedures such that calibration error would not bias towards one of the eye.

Among the 4 calibration procedures being studied in the experiment, the Stylus-mark calibration procedure is recommended. However, none of the four procedures can achieve a reliable and accurate result for naive user.

We suggest system designer to incorporate a two phase calibration procedure, where the SPAAM or its variant could be used for an initial coarse calibration, and some other mechanisms could be used to fine-tune the calibration.

## 7. Acknowledgement

We would like to thank Andrew Pariser for implementing the experimental setup and collecting data in the experiment. This work was supported by the National Science Foundation Grants #00-8274, #02-22831. This work is based on works performed under a grant from the Siemens Corporation.

## 8. Reference

1. Azuma, R., *A Survey of Augmented Reality*. Presence: Teleoperators and Virtual Environment, 1997. **6**(4): p. 355-385.
2. Barfield, W. and Caudell, T., *Basic Concepts in Wearable Computers and Augmented Reality*, in *Fundamentals of Wearable Computers and Augmented Reality*, Barfield, W. and Caudell, T., Editors. 2001, Lawrence Erlbaum Associates, Publishers: Mahwah, NJ.
3. Azuma, R., Baillet, Y., Behringer, R., Feiner, S., Julier, S., and MacIntyre, B., *Recent advances in augmented reality*. IEEE Computer Graphics and Applications, 2001. **21**(6): p. 34-47.
4. Rolland, J. and Fuchs, H., *Optical versus Video See-Through Head-Mounted Displays*, in *Fundamentals of Wearable Computers and Augmented Reality*, Barfield, W. and Caudell, T.P., Editors. 2001, Lawrence Erlbaum Associates, Publishers: Mahwah, NJ. p. 113-156.
5. Koller, D., Klinker, G., Rose, E., Breen, D., Whitaker, R., and Tuceryan, M. *Real-time vision-based camera tracking for augmented reality applications*, in *ACM Symposium on Virtual Reality Software and Technology*, 1997, Lausanne, Switzerland.
6. Azuma, R., *Predictive tracking for augmented reality*, in *Computer Science*. 1995, University of North Carolina, Chapel Hill: Chapel Hill, NC. p. 262.
7. Tuceryan, M. and Navab, N. *Single Point Active Alignment Method (SPAAM) for optical see-through HMD calibration*, in *IEEE and ACM International Symposium on Augmented Reality*, 149-158, Munich, Germany.
8. Genc, Y., Sauer, F., Wenzel, F., Tuceryan, M., and Navab, N. *Optical see-through HMD calibration: A stereo method validated with a video see-through system*, in *International Symposium for Augmented Reality*, 2000, Munich, Germany.
9. Owen, C., Tang, A., Zhou, J., and Xiao, F., *Blended Script and Compiled Code Development for Augmented Reality*. 2003. Technical Report: Michigan State University, East Lansing, MI.
10. Fuhrmann, A., Schmalstieg, D., and Purgathofer, W. *Fast Calibration for Augmented Reality*, in *ACM Symposium on Virtual Reality Software and Technology*, 1999, London, UK.
11. Fuhrmann, A., Schmalstieg, D., and Purgathofer, W. *Practical Calibration Procedures for Augmented Reality*, in *6th Eurographics Workshop on Virtual Environments*, 2000, Amsterdam, Netherlands.
12. McGarrity, E., Tuceryan, M., Owen, C., Genc, Y., and Navab, N. *Evaluation of Optical See-Through Systems*, in *Euroimage International Conference on Augmented, Virtual Environments and Three-Dimensional Imaging (ICAV3D)*, 2001, Mykonos, Greece.
13. McGarrity, E., Tuceryan, M., Tuceryan, M., Owen, C., and Navab, N. *A new system for online quantitative evaluation of optical see-through augmentation*, in *IEEE and ACM International Symposium on Augmented Reality*, 2001, New York, NY.
14. Heuvelmans, H.E.M., *A Typewriting system operated by head movements, based on home-computer equipment*. Applied Ergonomics, 1990. **21**(2): p. 115-120.
15. Bakic, V., *An interface for human-computer interaction based on face feature tracking in 2D*, in *Computer Science and Engineering*. 2000, Michigan State University: East Lansing. p. 277.
16. Fitts, P.M., *The information capacity of the human motor system in controlling amplitude of movement*. Journal of Experimental Psychology, 1954. **46**: p. 381-391.
17. Langolf, G.D., *Human motor performance in precise microscopic work*. 1973, University of Michigan, Ann Arbor: Ann Arbor, MI.
18. Card, S., Mackinlay, J., and Robertson, G. *The design space of input devices*, in *ACM CHI '90*, 1990, Seattle, WA.